

## Production of Ultracold NH Molecules by Sympathetic Cooling with Mg

Alisdair O. G. Wallis and Jeremy M. Hutson

*Department of Chemistry, Durham University, South Road, Durham, DH1 3LE, United Kingdom*

(Received 29 June 2009; published 28 October 2009)

We show that sympathetic cooling of NH molecules by Mg atoms has a good prospect of success. We carry out calculations on  $M$ -changing collisions of NH ( $^3\Sigma^-$ ) molecules in magnetically trappable states with Mg, using a recently calculated potential energy surface. We show that elastic collision rates are much faster than inelastic rates for a wide range of fields at temperatures up to 10 mK and that the ratio increases for lower temperatures and magnetic fields.

DOI: 10.1103/PhysRevLett.103.183201

PACS numbers: 37.10.Mn, 34.50.Cx, 37.10.Pq

There is great interest in the production of samples of cold molecules, at temperatures below 1 K, and ultracold molecules, at temperatures below 1 mK. Ultracold molecules have many potential applications in areas ranging from precision measurement to quantum computing. They also offer new possibilities for quantum control and controlled ultracold chemistry.

There have been considerable successes in producing ultracold molecules in laser-cooled atomic gases [1], both by photoassociation [2] and by magnetoassociation [3]. Ultracold KRb [4] and Cs<sub>2</sub> [5] have very recently been produced in their ground rovibrational states by magnetoassociation followed by stimulated Raman adiabatic passage (STIRAP). However, such methods are limited to molecules formed from atoms that can be laser-cooled, such as the alkali metals. A wider range of molecules can be cooled directly from high temperature to the millikelvin regime, using methods such as buffer-gas cooling [6] and Stark deceleration [7]. Low-field-seeking states of these cold molecules can then be confined in electrostatic and magnetic traps. However, at present the lowest temperature that can be achieved for directly cooled molecules in static traps is around 10 mK. The major challenge in this field is to find ways to cool such molecules to the ultracold regime.

One of the most promising proposals for second-stage cooling is *sympathetic cooling*, in which molecules are brought into contact with a laser-cooled atomic gas that is already ultracold. The hope is that thermalization will occur to produce ultracold molecules. However, atom-molecule potential energy surfaces are often strongly anisotropic and the anisotropy may drive fast inelastic collisions (relaxation). Such collisions may prevent sympathetic cooling, because they release kinetic energy and cause trap loss. A commonly stated rule of thumb is that elastic collisions must be at least a factor of 100 faster than inelastic collisions if sympathetic cooling is to succeed.

In previous work, we have used high-level electronic structure calculations to calculate interaction potentials for a variety of systems that are candidates for sympathetic cooling. The systems investigated include OH with Rb [8,9] and NH<sub>3</sub> and NH ( $^3\Sigma$ ) with alkali-metal and alkaline-earth-metal atoms [10,11]. Most of these systems

were found to have interaction potentials with deep wells and strong anisotropy, and several of them also have ion-pair states that are expected to cause additional inelasticity. It is unlikely that sympathetic cooling would work for molecules in low-field-seeking states in systems with high anisotropy. However, Mg + NH and Be + NH were found to be much less anisotropic and their ion-pair states are likely to be energetically inaccessible in low-energy collisions [11].

The purpose of the present Letter is to report for the first time a molecular system in which sympathetic cooling has a good prospect of success. We carry out quantum scattering calculations on Mg + NH and show that the ratio of elastic to inelastic cross sections is high enough to allow sympathetic cooling over a wide range of collision energies and magnetic fields.

Cold NH in its ground  $^3\Sigma$  state can be cooled in a helium buffer gas and confined in a magnetic trap [12,13], and laser cooling of Mg to sub-Doppler temperatures has recently been achieved [14]. NH can also be decelerated and trapped electrostatically in its excited  $^1\Delta$  electronic state [15,16] and there is a proposal to transfer the molecules to the ground state and accumulate them in a magnetic trap [17].

The energy levels of NH in a magnetic field are most conveniently described using Hund's case (b), in which the molecular rotation  $n$  couples to the spin  $s$  to produce a total monomer angular momentum  $j$ . In zero field, each rotational level  $n$  is split into sublevels labeled by  $j$ . In a magnetic field, each sublevel splits further into  $2j + 1$  levels labeled by  $m_j$ , the projection of  $j$  onto the axis defined by the field. For the  $n = 0$  levels that are of most interest for cold molecule studies, there is only a single zero-field level with  $j = 1$  that splits into three components with  $m_j = +1, 0$  and  $-1$ . Molecules in the  $m_j = +1$  state are low field seeking and can be confined in a magnetic trap, whereas those in the  $m_j = 0$  and  $-1$  states are untrapped.

The collisions that are of most interest are those of NH molecules that are initially in the magnetically trappable  $m_j = +1$  state, which may undergo inelastic collisions to untrapped states with  $m_j = 0$  and  $-1$ . We carry out quan-

tum scattering calculations of these collisions using the MOLSCAT package [18], as modified to handle collisions in magnetic fields [19]. The calculations are carried out in a partly coupled basis set  $|nsjm_j\rangle|LM_L\rangle$ , where  $L$  is the end-over-end rotational angular momentum of the Mg atom and the NH molecule about one another and  $M_L$  is its projection on the axis defined by the magnetic field. Hyperfine structure is neglected. The matrix elements of the total Hamiltonian in this basis are given in Ref. [19]. The only good quantum numbers during the collision are the parity  $p = (-1)^{n+L+1}$  and the total projection quantum number  $\mathcal{M} = m_j + M_L$ ; the total Hamiltonian is block diagonalized and scattering calculations are performed separately for each parity and  $\mathcal{M}$ . The calculations in the present work use basis sets with  $n_{\max} = 6$  and  $L_{\max} = 8$ .

MOLSCAT constructs a set of coupled equations in the intermolecular distance  $R$  and propagates them by the hybrid log-derivative method of Alexander and Manolopoulos [20], which uses a fixed-step-size log-derivative propagator in the short-range region ( $2.5 \leq R < 50$  Å) and a variable-step-size Airy propagator in the long-range region ( $50 \leq R \leq 250$  Å). The log-derivative solutions for each  $\mathcal{M}$  are then matched to asymptotic boundary conditions [21] to obtain the scattering matrix  $S^{\mathcal{M}p}$  and  $T$  matrix  $T^{\mathcal{M}p} = I - S^{\mathcal{M}p}$ . It is useful to decompose the integral cross sections between NH levels ( $|\alpha\rangle = |nsjm_j\rangle$ ) into sums of partial cross sections characterized by the  $L$  quantum number in the incident channel,

$$\sigma_{\alpha \rightarrow \alpha'}^L = \frac{\pi}{k_\alpha^2} \sum_{\mathcal{M}pL'} |T_{\alpha, LM_L \rightarrow \alpha', L'M_L'}^{\mathcal{M}p}|^2, \quad (1)$$

where  $M_L = \mathcal{M} - m_j$ ,  $M_L' = \mathcal{M} - m_j'$ ,  $k_\alpha$  is the wave vector for incoming channel  $\alpha$ , with collision energy  $E = \hbar^2 k_\alpha^2 / 2\mu$ , and  $\mu$  is the reduced mass of the colliding system. Since we focus here on transitions among the  $n = 0$ ,  $j = 1$  levels, we abbreviate the labels  $\alpha$  to just  $m_j$ . For molecules initially in the  $m_j = +1$  state, the most important quantities are the elastic and total inelastic cross sections; the latter is the sum of the state-to-state inelastic cross sections to the  $m_j = 0$  and  $m_j = -1$  states.

The mechanism of spin relaxation for  $^3\Sigma$  molecules has been studied extensively [22–26]. At sufficiently low energy, incoming channels with  $L > 0$  are suppressed by centrifugal barriers. The heights of the barriers are approximately  $E_{\text{cf}}^L = (\hbar L(L+1)/\mu)^{3/2} (54C_6)^{-1/2}$ , which is 23 mK for Mg + NH with  $L = 2$ . For  $L = 0$  ( $s$ -wave scattering),  $M_L = 0$  and hence  $\mathcal{M} = m_j$ . Since  $\mathcal{M}$  is conserved there is no outgoing channel with  $L' = 0$  for  $m_j' = 0$  or  $-1$  and the dominant relaxation channels for  $s$ -wave scattering have  $L' = 2$  in the outgoing channels.

The coupling between channels with different  $m_j$  occurs via the interplay of the spin-spin interaction and the potential anisotropy. The spin-spin term in the NH Hamiltonian mixes the  $n = 0$  and  $n = 2$  states with the

same  $j$  and  $m_j$ , and the potential anisotropy then mixes states of different  $L$  such that  $\Delta m_j + \Delta M_L = 0$ .

In the absence of a magnetic field, the thresholds for different values of  $m_j$  are degenerate. The presence of centrifugal barriers in the outgoing channels strongly suppresses the inelastic transitions, but the spin-relaxation cross section is nevertheless nonzero at finite energy [23,24]. Application of a magnetic field removes the degeneracy, increasing the kinetic energy in the outgoing channels and reducing the centrifugal suppression. By contrast, the elastic cross section is dominated by  $\Delta L = 0$  collisions so is almost field independent.

Figure 1 shows the  $s$ -wave elastic cross section  $\sigma_{\Delta m_j=0}^0$  and the total inelastic cross section  $\sigma_{\Delta m_j \neq 0}^0$  for initial  $m_j = +1$  as a function of energy for varying magnetic field strengths, while Fig. 2 shows the  $s$ -wave total inelastic cross sections as a function of magnetic field for a number of different collision energies. It may be seen that the total inelastic cross section in the ultracold regime decreases dramatically as the magnetic field is reduced.

Volpi and Bohn [22] have given a simple one-parameter formula for the threshold behavior of the inelastic cross sections as a function of energy and magnetic field. They obtained

$$\sigma_{\alpha L \rightarrow \alpha' L'}(E, B) = \sigma_{\alpha\alpha'}^{LL'} E^{L-(1/2)} (E + \Delta m_j g \mu_0 B)^{L'+(1/2)}, \quad (2)$$

where the factor  $\sigma_{\alpha\alpha'}^{LL'}$  is independent of energy and magnetic field,  $\Delta m_j g \mu_0 B$  is the linear Zeeman shift with  $\Delta m_j = m_j - m_j'$ ,  $g$  is the electron  $g$ -factor, and  $\mu_0$  is the Bohr magneton. For Mg + NH, the  $s$ -wave ( $L = 0 \rightarrow L' = 2$ ) inelastic cross sections follow Eq. (2) for collision energies up to about  $10^{-4}$  K. When the collision energy is less than the Zeeman shift, this gives a cross section

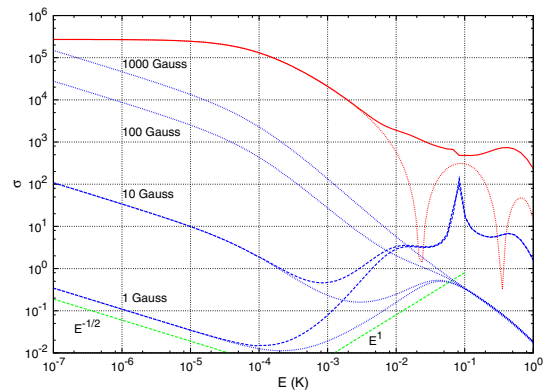


FIG. 1 (color online). Mg + NH elastic (red) and inelastic (blue) cross sections (in Å<sup>2</sup>) as a function of collision energy for various magnetic fields. The dotted curves show  $s$ -wave cross sections,  $\sigma_{m_j=+1 \rightarrow +1}^{L=0}$  (elastic) and  $\sigma_{m_j=+1 \rightarrow 0}^{L=0} + \sigma_{m_j=+1 \rightarrow -1}^{L=0}$  (total inelastic). The solid and dashed curves show integral cross sections including  $p$ ,  $d$  and  $f$  waves ( $L = 1, 2$  and  $3$ ), which gives convergence for energies up to 100 mK. The dashed green lines show  $E^{-1/2}$  and  $E^1$  behavior.

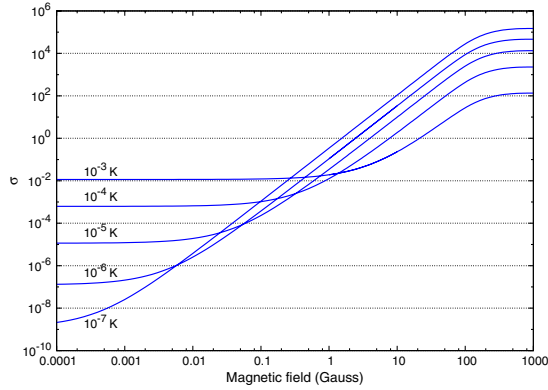


FIG. 2 (color online). Mg + NH total inelastic  $s$ -wave cross sections  $\sigma_{m_j=+1 \rightarrow 0}^{L=0} + \sigma_{m_j=+1 \rightarrow -1}^{L=0}$  (in  $\text{\AA}^2$ ) as a function of magnetic field strength for various collision energies.

proportional to  $E^{-1/2}$ . However,  $E^2$  behavior at higher energies occurs only for fields below 0.1 G, when the kinetic energy in the outgoing channel is also below  $10^{-4}$  K. At the higher fields shown in Fig. 1, the rising limb of the  $s$ -wave cross section is closer to  $E^1$ .

At low enough magnetic field, all the  $s$ -wave inelastic cross sections in Fig. 2 flatten out to a zero-field value proportional to  $E^2$ . At higher field they enter a region of  $B^{5/2}$  dependence. This continues until the centrifugal barrier is exceeded in the outgoing channel and the cross sections then flatten off with a value proportional to  $E^{-1/2}$ .

As mentioned in the Introduction, the general rule of thumb for sympathetic cooling to work is that the ratio  $\gamma$  of elastic to total inelastic cross sections must be greater than about 100. It can be seen in Fig. 1 that for small magnetic fields and low collision energies  $\gamma$  is well in excess of 100. However, at collision energies above  $\sim 10^{-4}$  K, higher partial waves start contributing significantly to the total cross sections. The total cross sections incorporating additional  $p$ ,  $d$ , and  $f$  partial waves ( $L = 1, 2$  and  $3$ ) are included in Fig. 1 for 1 and 10 G. There is a sharp peak in the  $d$ -wave inelastic cross section around 75 mK, but everywhere else  $\gamma$  remains in excess of 100 until partial waves with  $L = 4$  become important above 100 mK.

In order to assess the prospects of sympathetic cooling for NH with Mg, Fig. 3 shows a contour plot of  $\gamma$  as a function of collision energy and magnetic field strength. At the top left of this figure, inelastic collisions are too fast for sympathetic cooling to succeed. However, in an unbiased magnetic trap with zero field at the center, trapped molecules in  $m_j = +1$  states at temperature  $T$  will be distributed according to a Boltzmann distribution with density  $\rho$  given by

$$\rho/\rho_0 = \exp\left(\frac{-m_j g \mu_0 B}{k_B T}\right). \quad (3)$$

At any given temperature on the energy axis of Fig. 3, only about 0.1% of molecules will experience fields greater than  $B = 6k_B T/g\mu_0$ , which is shown as a red line in Fig. 3.

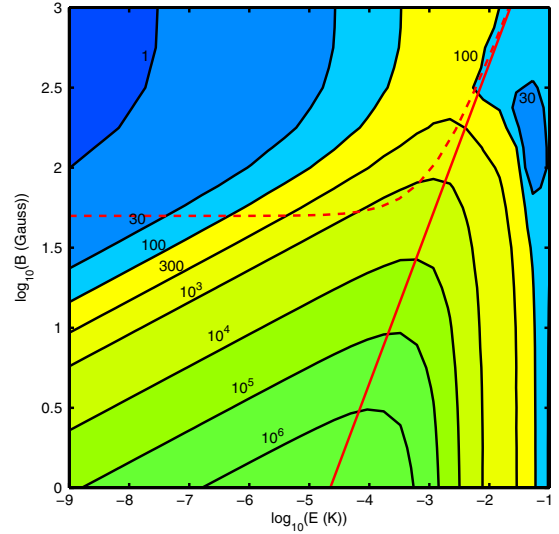


FIG. 3 (color online). Contour plot of the ratio  $\gamma$  of elastic to total inelastic cross sections as a function of magnetic field strength and collision energy. The red lines show the maximum field sampled by trapped molecules in the  $m_j = +1$  state ( $B = 6kT/g\mu_0$ ) in an unbiased trap (solid line) and for a trap with a bias field of 50 G (dashed line).

Most molecules in a magnetic trap will experience fields below this line.

A precooled sample of molecules would initially have a temperature on the order of tens of milliKelvin. For temperatures up to about 10 mK,  $\gamma$  is always greater than 100 in the thermally allowed region. Even above this,  $\gamma$  remains close to 100. Nevertheless, it will be important to precool the molecules as much as possible before sympathetic cooling begins. As the sample is cooled towards sub-mK temperatures, the maximum magnetic field strength sampled by the molecules decreases,  $\gamma$  increases and the trapped NH molecules become increasingly stable to collisional spin relaxation.

Trapped atoms and molecules may undergo nonadiabatic transitions when they pass through regions of space where different levels are degenerate. This is a particular problem for quadrupole traps, which have zero field at the trap center: a molecule that passes close to the center experiences a very fast change in the field direction that may cause spin-flip transitions [27,28] and lead to trap loss. For this reason, many experiments on ultracold atoms use traps with a nonzero magnetic field at the center, and similar designs have also been explored for molecules in electrostatic traps [29]. For atomic systems, a bias field of 1 G or less is usually sufficient to prevent nonadiabatic losses. However, for  $^{14}\text{NH}$  there are 6 magnetically trapable hyperfine levels. Three of these correlate with the highest zero-field level, with total angular momentum  $F = 3/2$ , and are not subject to level crossings as a function of field. The other three correlate with  $F = 5/2$  and cross untrapped states at fields between 18 and 32 G. It may therefore be necessary to apply a larger bias field to avoid

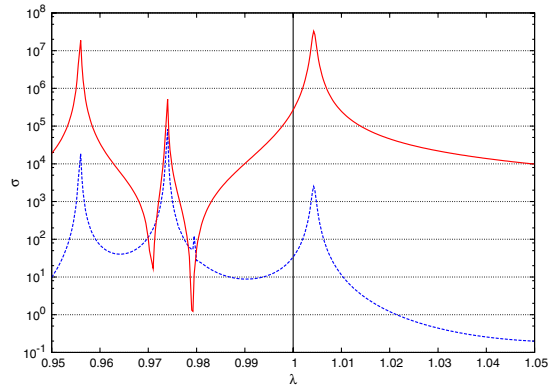


FIG. 4 (color online).  $S$ -wave elastic (solid, red) and total inelastic (dashed, blue) cross sections (in  $\text{\AA}^2$ ) as a function of the potential scaling factor  $\lambda$ , calculated for a collision energy of  $10^{-6}$  K at a magnetic field of 10 G.

one-body losses for NH. The dashed red line in Fig. 3 shows the upper limit of the fields explored by molecules in a trap with a bias field of 50 G. Even a bias field this large causes very little change in the temperature at which sympathetic cooling begins, and it is still possible to cool the molecules below 1  $\mu\text{K}$  before inelastic losses become significant.

Scattering at low energy depends strongly on the details of the potential energy surface. The potential energy surface used in the present work is probably accurate to about 5%. To explore whether uncertainty in the potential surface affects our conclusions, we consider the effect of a scaling factor  $\lambda$  that produces a modified potential energy surface  $V^{\text{scaled}}(R, \theta) = \lambda V(R, \theta)$ . The  $s$ -wave elastic and total inelastic cross sections are shown as a function of  $\lambda$  in Fig. 4 for a collision energy of 1  $\mu\text{K}$  at a field of 10 G. Both the elastic and inelastic cross sections show strong resonance structures as Mg-NH bound and quasibound states cross the low-field-seeking threshold as the potential is varied. However, away from the strong resonant structures the ratio of elastic to inelastic cross sections remains large. This indicates that our conclusions are reasonably independent of the details of the potential energy surface and confirms that Mg is a good candidate for sympathetic cooling of magnetically trapped NH.

In conclusion, we have carried out calculations on spin-changing collisions for  $\text{NH}(\Sigma^-)$  molecules colliding with Mg atoms. We find that the ratio of elastic to inelastic cross sections exceeds 100, the factor required for sympathetic cooling to succeed, for a wide range of collision energies and magnetic fields. If precooled NH molecules at a temperature around 10 mK can be brought into contact with laser-cooled Mg, there is a good prospect that sympathetic cooling will succeed. The inelastic losses decrease even further as the temperature decreases, so that once sympathetic cooling begins it will continue.

The authors are grateful to EPSRC for financial support for AOGW and for funding the collaborative project

CoPoMol under the ESF EUROCORES programme EuroQUAM.

- [1] J. M. Hutson and P. Soldán, *Int. Rev. Phys. Chem.* **25**, 497 (2006).
- [2] K. M. Jones, E. Tiesinga, P. D. Lett, and P. S. Julienne, *Rev. Mod. Phys.* **78**, 483 (2006).
- [3] T. Köhler, K. Goral, and P. S. Julienne, *Rev. Mod. Phys.* **78**, 1311 (2006).
- [4] K.-K. Ni, S. Ospelkaus, M. H. G. de Miranda, A. Pe'er, B. Neyenhuis, J. J. Zirbel, S. Kotochigova, P. S. Julienne, D. S. Jin, and J. Ye, *Science* **322**, 231 (2008).
- [5] J. G. Danzl, M. J. Mark, E. Haller, M. Gustavsson, R. Hart, J. Aldegunde, J. M. Hutson, and H.-C. Nägerl, arXiv:0909.4700.
- [6] J. D. Weinstein, R. deCarvalho, T. Guillet, B. Friedrich, and J. M. Doyle, *Nature (London)* **395**, 148 (1998).
- [7] H. L. Bethlem and G. Meijer, *Int. Rev. Phys. Chem.* **22**, 73 (2003).
- [8] M. Lara, J. L. Bohn, D. Potter, P. Soldán, and J. M. Hutson, *Phys. Rev. Lett.* **97**, 183201 (2006).
- [9] M. Lara, J. L. Bohn, D. E. Potter, P. Soldán, and J. M. Hutson, *Phys. Rev. A* **75**, 012704 (2007).
- [10] P. S. Żuchowski and J. M. Hutson, *Phys. Rev. A* **78**, 022701 (2008).
- [11] P. Soldán, P. S. Żuchowski, and J. M. Hutson, *Faraday Discuss.* **142**, 191 (2009).
- [12] D. Egorov, W. C. Campbell, B. Friedrich, S. E. Maxwell, E. Tsikata, L. D. van Buuren, and J. M. Doyle, *Eur. Phys. J. D* **31**, 307 (2004).
- [13] W. C. Campbell, E. Tsikata, H.-I. Lu, L. D. van Buuren, and J. M. Doyle, *Phys. Rev. Lett.* **98**, 213001 (2007).
- [14] T. E. Mehlstäubler, K. Moldenhauer, M. Riedmann, N. Rehbein, J. Friebe, E. M. Rasel, and W. Ertmer, *Phys. Rev. A* **77**, 021402(R) (2008).
- [15] S. Y. T. van de Meerakker, I. Labazan, S. Hoekstra, J. Küpper, and G. Meijer, *J. Phys. B* **39**, S1077 (2006).
- [16] S. Hoekstra *et al.*, *Phys. Rev. A* **76**, 063408 (2007).
- [17] S. Y. T. van de Meerakker, R. T. Jongma, H. L. Bethlem, and G. Meijer, *Phys. Rev. A* **64**, 041401(R) (2001).
- [18] J. M. Hutson and S. Green, *MOLSCAT Computer Program, Version 14* (CCP6, Daresbury, 1994).
- [19] M. L. González-Martínez and J. M. Hutson, *Phys. Rev. A* **75**, 022702 (2007).
- [20] M. H. Alexander and D. E. Manolopoulos, *J. Chem. Phys.* **86**, 2044 (1987).
- [21] B. R. Johnson, *J. Comput. Phys.* **13**, 445 (1973).
- [22] A. Volpi and J. L. Bohn, *Phys. Rev. A* **65**, 052712 (2002).
- [23] R. V. Krems *et al.*, *Phys. Rev. A* **68**, 051401(R) (2003).
- [24] R. V. Krems and A. Dalgarno, *J. Chem. Phys.* **120**, 2296 (2004).
- [25] H. Cybulski, R. V. Krems, H. R. Sadeghpour, A. Dalgarno, J. Kłos, G. C. Groenenboom, A. van der Avoird, D. Zgid, and G. Chałasiński, *J. Chem. Phys.* **122**, 094307 (2005).
- [26] W. C. Campbell *et al.*, *Phys. Rev. Lett.* **102**, 013003 (2009).
- [27] E. Majorana, *Nuovo Cimento* **9**, 43 (1932).
- [28] W. Petrich, M. H. Anderson, J. R. Ensher, and E. A. Cornell, *Phys. Rev. Lett.* **74**, 3352 (1995).
- [29] M. Kirste, B. G. Sartakov, M. Schnell, and G. Meijer, *Phys. Rev. A* **79**, 051401(R) (2009).